Transverse wall instabilities on a driven, damped two-dimensional lattice system

J. Pouget,* S. Aubry,† A. R. Bishop, and P. S. Lomdahl
Center for Nonlinear Studies and Theoretical Division, Los Alamos National Laboratory, Los Alamos, New Mexico 87545
(Received 26 February 1988; revised manuscript received 27 December 1988)

Analytic and numerical studies are presented for the onset and saturation of transverse patterns occurring on walls propagating in a two-dimensional, longitudinally discrete, underdamped, dc-driven Frenkel-Kontorova model. For sufficiently weak damping, transverse instabilities occur at a series of critical field thresholds, where the wall velocity is of intermediate magnitude. Typically, the transverse patterns saturate as counterpropagating kink-antikink pairs, whose nucleation supports the longitudinal wall propagation. The wall dynamics in a D-dimensional lattice is governed approximately by a damped drive $(D-1)$-dimensional sine-Gordon equation.

I. INTRODUCTION

Pattern formation and dynamics are central themes of current research in extended dynamical systems, with important consequences for physical properties, especially transport, in many diverse contexts. In this paper we study the onset and nonlinear saturation of transverse patterns occurring on walls propagating in a two-dimensional, longitudinally *discrete,* dc-driven Frenkel-Kontorova model. Results of a direct numerical simulation are compared with an approximate analysis which suggests that a moving flat wall in a two-dimensional (2D) or 3D lattice should be unstable with respect to the transverse fluctuations if the damping is small enough.

This is an excellent example of transverse instability and nonlinear saturation into dynamic patterns occurring on a longitudinally propagating interface. A similar phenomenon is manifested in many different contexts of passive or active interfaces[1]—e.g., commensurately pinned charge-density waves;[2] vortex lattices in superconducting films with periodically modulated thickness;[3] dislocations in atomic lattices,[4-5] ferromagnets, ferroelectrics, large Josephson junctions, or junction arrays; cellular patterns on moving fluid or frame fronts; dendritic patterns on solid-liquid interfaces.

Some analytic results are already available, particularly in Frenkel-Kontorova or Φ^4 models, but the discreteness effects are generally considered as small perturbations.[6-11] On the other hand, studies of continuum ac- and dc-driven, damped sine-Gordon systems have revealed space-time pattern formation whose mechanism is quite similar to that of the present work.[12,13] This similarity is because a moving wall in a lattice is subject to a periodic Peierls-Nabarro pinning force. More precisely, (see Section II) the location of the wall in the propagation direction depends then on the time and a transverse center-of-mass collective variable. Such a periodic pinning force does not occur in purely continuum models since the amplitude of the Peierls-Nabarro barrier approaches zero (exponentially) as a function of increasing wall thickness relative to a lattice spacing. It is well known that discreteness effects are responsible for qualitatively new phenomena, such as wall pinning and structural chaos.[14-16] As explained in Sec. II these instabilities are parametric instabilities occurring beyond a some critical amplitude of the Peierls-Nabarro barrier in a range where the discreteness effects dominate. As might be anticipated, transverse structure occurs when the driving force is sufficient to depin the wall. Within the 2D model considered here the instabilities appear as nucleation of kink-antikink pairs propagating transversely and (for periodic boundary conditions in the tranverse direction) persistently with a density determined by the strength of the driving field. Related transverse instabilities have also been observed in *two-* component displacement Frenkel-Kontorova models supporting both edge and screw dislocations.[17]

Section II established our central Frenkel-Kontorova model with a uniaxial lattice displacement, including damping and driving. Considering a single moving 2π domain wall, an approximate stability analysis is developed by mapping the D-dimensional problem to a $(D-1)$-dimensional one for a local wall collective coordinate. This effective problem has the form of a driven, damped sine-Gordon equation. Numerical experiments for the 2D case are presented in Sec. III for several combinations of the relevant parameters (domain wall thickness and the strengths of damping and driving). The approximate analytic analysis is confirmed and additional phenomena [e.g. formation of double (4π) walls] are identified at large driving strengths, where the longitudinal wall structure and bound-state oscillations become important. Section IV contains a summary and discussion.

II. PARAMETRIC INSTABILITY OF A MOVING WALL IN THE DISCRETE SINE-GORDON MODEL

We consider a moving wall in a three-dimensional lattice. [The following analysis extends trivially to a $(D-1)$-dimensional wall in a D-dimensional lattice.] The motion of this wall can be derived from the following Lagrangian:

$$\mathcal{L}=\sum_{i,j,k}{}'[\tfrac{1}{2}\dot{\Phi}_{i,j,k}^2-\tfrac{1}{2}K_L(\Phi_{i+1,j,k}-\Phi_{i,j,k})^2 -\tfrac{1}{2}K_{T_x}(\Phi_{i,j+1,k}-\Phi_{i,j,k})^2 -\tfrac{1}{2}K_{T_y}(\Phi_{i,j,k+1}-\Phi_{i,j,k})^2 -K(1-\cos\Phi_{i,j,k})] , \tag{1}$$

where $\Phi_{i,j,k}$ is the displacement at lattice site (i,j,k), K_L is the longitudinal lattice constant, K_{T_x} and K_{T_y} are the transverse lattice constants in the x direction and y direction, respectively, and K is the strength of the potential. Since the moving wall will be subject to a periodic Peierls-Nabarro pinning force (see below), we may anticipate instabilities in the transverse directions. For the purposes of an analytic approximation, we assume here that the transverse Peierls-Nabarro barrier is weak. This means that the characteristic lengths of transverse disturbances are large enough that the transverse directions can be treated continuously. A finite Peierls-Nabarro barrier in the *longitudinal* z direction is essential for the following instability process. Taking the displacement field $\Phi_{i,j,k}$ to depend continuously on transverse coordinates x and y, the Lagrangian (1) can be rewritten as

$$\mathcal{L}=\int_{\mathbb{R}^2}\left[\sum_i\tfrac{1}{2}\dot{\Phi}_i^2-\tfrac{1}{2}K_L(\Phi_{i+1}-\Phi_i)^2-\tfrac{1}{2}K_{T_x}\left[\frac{\partial\Phi_i}{\partial x}\right]^2 -\tfrac{1}{2}K_{T_y}\left[\frac{\partial\Phi_i}{\partial y}\right]^2,-K(1-\cos\Phi_i)\right]dx\,dy . \tag{2}$$

From the Lagrangian (2) we can deduce the equations governing the displacement field Φ_i which is continuous with respect to (x,y) discretized in the z direction

$$\ddot{\Phi}_i=K_L(\Phi_{i+1}+\Phi_{i-1}-2\Phi_i)+K_{T_x}\Phi_{i,xx} +K_{T_y}\Phi_{i,yy}-K\sin\Phi_i-\gamma\dot{\Phi}_i-F . \tag{3}$$

Here dissipation (strength γ) and a constant uniform force have been included. Introducing the change of variables

$$\tau=\sqrt{K_L}\,t,\quad X=\left[\frac{K_L}{K_{T_x}}\right]^{1/2}x ,\quad Y=\left[\frac{K_L}{K_{T_y}}\right]^{1/2}y , \tag{4a}$$

and setting

$$\lambda=K/K_L,\quad \Gamma=\gamma/\sqrt{K_L},\quad G=F/K_L , \tag{4b}$$

Eq. (3) becomes

$$\Phi_{i,\tau\tau}=\Phi_{i+1}+\Phi_{i-1}-2\Phi_i+\Phi_{i,XX} +\Phi_{i,YY}-\lambda\sin\Phi_i-\Gamma\Phi_{1,\tau}-G . \tag{5}$$

We now assume that Γ is a small damping constant and G a small dc driving force. In addition the coupling constant λ between the lattice and the periodic potential is also assumed to be small. With these conditions, the distorted wall can reasonably be approximated by the ansatz

$$\Phi_i(X,Y,\tau)=4\tan^{-1}(\exp\mu\xi_i) , \tag{6a}$$

with

$$\xi_i=i-U(X,Y,\tau) , \tag{6b}$$

$$\mu=[\lambda/(1-V^2)]^{1/2} , \tag{6c}$$

$$V(X,Y,\tau)=\frac{\partial}{\partial\tau}U(X,Y,\tau) . \tag{6d}$$

Ansatz (6) is motivated by the well-known exact-wall (soliton) solution to the one-dimensional sine-Gordon equation. The wall deformation is now described by a continuous function $U(X,Y,\tau)$ which represents the position of the wall along the lines parallel to the z direction at time τ. In the continuum limit the wall, of course, remains flat and the wall velocity is therefore independent of X, Y, and τ. The derivation of an approximate equation governing the dynamic of the wall location $U(X,Y,\tau)$ is given in Appendix A. The result is

$$\Psi_{\tau\tau}-\Psi_{XX}-\Psi_{YY}+B\sin\Psi=-\Gamma\Psi_\tau-F , \tag{7}$$

where

$$F=\pi^2G/2\sqrt{\lambda} , \tag{8a}$$

and

$$B=\frac{8\pi^4}{\sqrt{\lambda}\sinh(\pi^2/\sqrt{\lambda})} , \tag{8b}$$

with

$$\Psi=2\pi U . \tag{8c}$$

From (7) we see that the wall location is described by a damped-driven sine-Gordon equation for a *two-* dimensional continuous system. The instabilities of the uniform wall occur when the coefficient B is large enough compared to the damping constant Γ. This means that the wall thickness in the discrete direction must be small enough, producing a large Peierls barrier.

Stability analysis

The uniform motion of the wall is described by a space-independent displacement field which, for $\Gamma=0$ and $F=0$ can be written in the form

$$\Psi_0(X,Y,\tau)=2\pi v\tau=g(2\pi v\tau) , \tag{9}$$

where $g(x)$ is some 2π periodic function and v is the average velocity of the wall. On considering small perturbations $\varepsilon(X,Y,\tau)$ about the solution Ψ_0,

$$\Psi(X,Y,\tau)=\Psi_0(\tau)+\varepsilon(X,Y,\tau) , \tag{10}$$

the equation for ε in linear order is

$$\ddot{\varepsilon}=\varepsilon_{XX}+\varepsilon_{YY}-a(2\pi v\tau)\varepsilon-\Gamma\dot{\varepsilon} , \tag{11}$$

where

$$a(x)=B\cos[x+g(x)] \tag{12}$$

is a 2π periodic function. Equivalently , in Fourier space we have

$$\ddot{\varepsilon}_q+\Gamma\dot{\varepsilon}_q+[|\mathbf{q}|^2+a(2\pi v\tau)]\varepsilon_q=0 \tag{13a}$$

with

$$\varepsilon_q(\tau)=\int \varepsilon(\mathbf{r},\tau)e^{i\mathbf{q}\cdot\mathbf{r}}d\mathbf{r} \ . \tag{13b}$$

For a given wave vector $\mathbf{q}$, Eq. (13a) is a parametric equation. The latter can be viewed as the one-dimensional Schrödinger equation for a quantum particle in the periodic potential $a(2\pi v\tau)$, where τ represents a space variable and $|q|^2$ is the eigenenergy. Stability requires that the solution of Eq. (13a) remain bounded for all time. The corresponding spectrum of the quantum particle contains an infinite series of gaps (for $\Gamma=0$) which are opened in the vicinity of the values

$$q_n=n\pi v \ . \tag{14}$$

Thus most solutions of the eigenvalue problem (13a) diverge when τ becomes large. In conclusion, we can say that in the *absence of damping* the uniform motion of a wall is always unstable against transverse fluctuations with wave vectors $\mathbf{q}$ of modulus close to q_n given by Eq. (14).

When the damping is nonzero. the stability analysis is more complicated and a perturbative treatment for the Floquet analysis for Eq. (13a) is necessary. For $\Gamma\neq 0$ but small, the main instability of the moving wall is obtained in first order [see Appendix B, Eq. (B10) for the wave vector

$$|q|=(n^2v^2+\Gamma^2/4)^{1/2} \tag{15a}$$

when

$$\Gamma<|a_1|/\pi v \ , \tag{15b}$$

where a_1 is the first Fourier coefficient of $a(x)$ (see Appendix B). Since $g(x)$ in Eq. (13) approaches zero as v tends to zero, the first Fourier coefficient of $a(x)$ has modulus $B/2$. Therefore, we find that for large velocity the flat wall in the discrete lattice is stable. Conversely, we expect from Eq. (15b) that the wall is always unstable below some critical velocity. Nevertheless the perturbation analysis [see Appendix B, Eq. (B11)] gives the restriction

$$v^2\gg\frac{|a_1|}{2\pi\sqrt{2}} \ . \tag{16}$$

This means that below a certain critical velocity v_c, at which the instabilities occur, the wall becomes "wrinkled" and the moving wall can exhibit complex patterns and bifurcations.

Elsewhere[13] we have studied the 1D reduced problem arising from an original 2D problem. This is of interest in its own right, e.g., for studying zero-field steps on annular Josephson junctions,[18] and provides examples of pattern formation and competition and of hysteretic transitions. The saturated patterns are either standing waves (breather wave trains) or bifurcations into transversely propagating kink-antikink pairs, whose density decreases in steps as the driving force is decreased. We will find in Sec. III that the nucleation of transverse kink-antikink pairs is indeed a common mechanism for supporting longitudinal wall dynamics—as in models of dislocation dynamics.[1] In higher dimensions, the saturated transverse patterns will be determined similarly by the transverse geometry and boundary conditions.

A special case: moving wall in 2D lattice

In preparation for performing numerical simulations, we present the basic equations for the 2D lattice system. Then Eq. (3) reduces to

$$\begin{aligned}\ddot{\Phi}_{i,j}=&K_L(\Phi_{i+1,j}+\Phi_{i-1j}-2\Phi_{ij})\\&+K_T(\Phi_{i,j+1}+\Phi_{i,j-1}-2\Phi_{i,j})\\&-K\sin\Phi_{i,j}-\gamma\dot{\Phi}_{i,j}-F \ ,\end{aligned} \tag{17}$$

where now K_T is the single transverse lattice parameter. The wall location depends only on X and τ and satisfies

$$\Psi_{TT}-\Psi_{XX}+\sin\Psi=-\hat{\Gamma}\Psi_T-\hat{F} \ , \tag{18}$$

where we have introduced

$$T=(K_LB)^{1/2}t \ , \tag{19a}$$

$$X=\left[\frac{K_LB}{K_T}\right]^{1/2}x \ , \tag{19b}$$

$$\Psi=2\pi U \ , \tag{19c}$$

and the effective coefficients are defined by

$$\hat{\Gamma}=\gamma/K_L\sqrt{B} \ , \tag{19d}$$

$$\hat{F}=\frac{\pi^2F}{2K_LB\sqrt{KK_L}} \ . \tag{19e}$$

The strength of the Peierls-Nabarro barrier B is given by Eq. (8b). Equation (18) is a normalized damped-driven sine-Gordon equation for a *one*-dimensional system which describes the dynamics of the kink location in the transverse direction. In this way, we have established an approximate mapping between the full equation (17) and an equation for the kink location.

III. NUMERICAL SIMULATIONS

The two-dimensional system used for our numerical simulation consists of a square lattice with 30×30, lattice points and anisotropic lattice constants. The initial condition is given by Eq. (2) and is shown in Fig. 1. However, in order to break the ideal symmetry of the initial condition, we have added small amplitude random noise. The transverse instabilities can thus be excited more easily. Periodic boundary conditions (modulo 2π) are imposed in the longitudinal direction. The typical parameters [see Eq. (17)] are chosen with respect to those of the normalized equation (18). For our numerical studies, we take $K=1$ and K_L and K_T control the characteristic

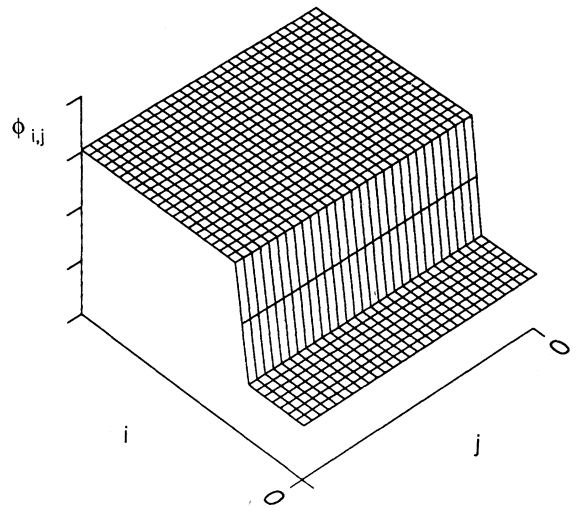

FIG. 1. Perspective plot of a flat 2π-wall initial condition with $K_L=0.335$. Periodic boundary conditions (modulo 2π in the longitudinal direction).

lengths in the longitudinal and transverse directions, respectively, K_L is associated with the wall thickness

$$\delta_x=\pi\left[\frac{K_L}{K}\right]^{1/2}, \tag{20}$$

and K_T similarly controls the width of transverse structure. The single wall corresponding to a solution of Eq. (18) has a width defined by

$$\Delta=\pi\left[\frac{K_T}{K_L B}\right]^{1/2}. \tag{21}$$

In the present study two values of K_L have been considered leading to two different wall thicknesses. The value of K_T is chosen such that Δ is of the order 5. We have taken $\hat{\Gamma}=0.09-0.08$ and $\hat{F}$ lies in the range $0.75-1.1$. K_L is such that δ_x is the order of 1.8 yielding $K_L=0.335$. With this value we estimate the Peierls-Nabarro barrier to be $B\simeq 3$.

If the force is too low the wall does not move and transverse structures are not generated. If the force is too high, nucleation of an additional wall-antiwall sequence behind the primary wall can occur, resulting in the formation of a "double layer".[16,17] Figure 2 gives the contour curves of the wall at level π. A perfectly flat wall (without transverse structure) then appears as a straight line. In Fig. 2(a) (where $\hat{F}=1.1$, an intermediate value) a transverse kink-antikink pair is evident. This pair collapses during collision and then reappears after collision. Because of the periodic boundary conditions in the transverse direction, the kink-antikink pair propagates around the contour line and the process can persist indefinitely, except for intrinsic dissipation because of transverse discreteness which can slowly transfer energy to phonon modes.

Impurities in the lattice can also trigger the transverse

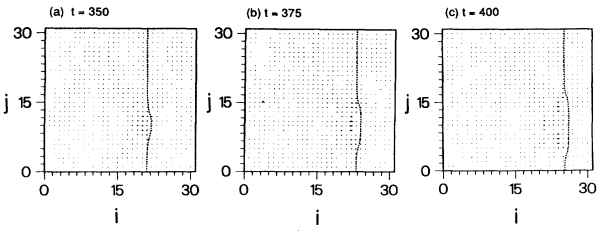

FIG. 2. Contour plots of $\Phi_{i,j}$. The dashed line indicates mod(π) displacement (i.e., the center of the wall). The size of the dots and arrows indicate the particle velocity. With the initial condition of Fig. 1, damping $\hat{\Gamma}=0.085$, and force $\hat{F}=1.1$, a single transverse kink-antikink pair is nucleated, as shown at the three successive times t (a), (b), and (c).

patterns. Figure 3 ($\hat{F}=1.1$) shows the transverse structure developed in the presence of three impurities lying on the lattice diagonal. The impurities were introduced as enhancements of local potentials, viz., $K=10$ at the three impurity sites. In this case, the structure seems to evolve symmetrically in the transverse direction. Note that the transverse structure does not interact again with these impurities after the kink-antikink nucleation. The arrows placed at each lattice point denote local velocities. During the nucleation process the velocities at the lattice points near the nucleation center are high. The evolution of the total energy is slowly oscillating and decreasing, this is due to the discretness effect and the dissipation contribution. Figure 4 ($\hat{F}=1.1$) gives a perspective plot of the square lattice, where the transverse structure is clearly exhibited on the wall; some phonon radiation is also propagating in both directions, presumably caused by the discretness. The phonon radiation in the longitudinal direction emitted when a particle jumps from one stable position of the substrate potential to the next one is now a well-understood phenomenon in the 1D Frenkel-Kontorova model.[7-9].

When the force $\hat{F}$ is increased beyond $\simeq 1.1$, large instabilities are generated which, in turn, create loop nucleations moving and collapsing behind the kink. This process generates new walls and is illustrated in Fig. 5.

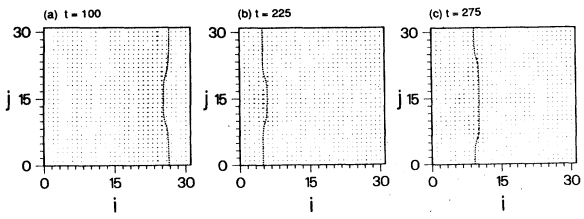

FIG. 3. Transverse structure in the presence of local impurities (see text). Here three impurities of strength $K=10.0$ are spaced equally along the diagonal. Other conditions are as in Fig. 2. In this case the impurities do not seriously inhibit transverse kink-antikink pair propagation and do not nucleate additional pairs.

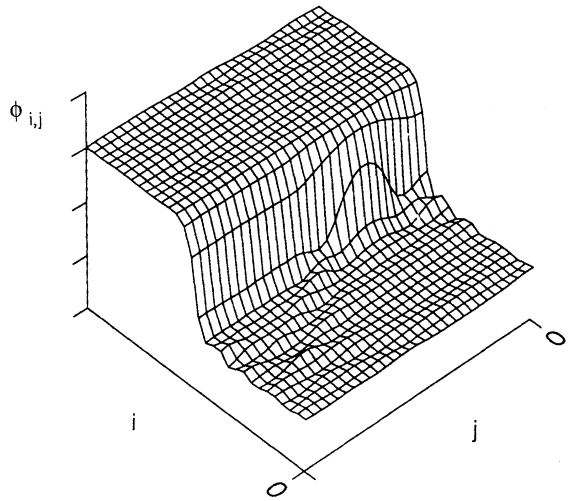

FIG. 4. Perspective plot of a representative propagating wall showing. (1) Nucleation of transverse instability (which will saturate as a kink-antikink pair); and (ii) associated phonon field initiated at the nucleation site and propagating in the wall's wake.

Finally we have considered a less discrete case, viz., a larger K_L such that $\delta x \simeq 2$. In this case the results are somewhat different—although the effective damping is the same as in the previous case and the forces are in the same range, the Peierls-Nabarro barrier is smaller. Here we have been able to nucleate *two* persistent kink-antikink pairs. Figure 6 (where $\hat{F}=0.9$) shows two such pairs moving in opposite directions. The pairs collide almost elastically and continue propagating transversely. In this case the Peierls-Nabarro barrier is $B=1.85$ which is a little more than half its value in the previous case. Cooresponding, the anisotropic ratio K_T/K_L is 7.5 and 3.8 in the first and second cases, respectively.

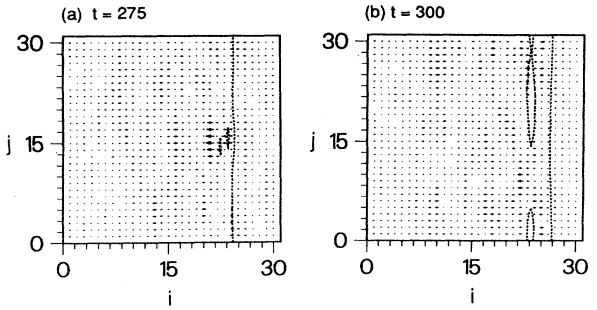

FIG. 5. Same conditions as Fig. 2. except that the driving force is $\hat{F}=1.2$. For $\hat{F} \gtrsim 1.1$ large-scale instabilities result in loops (i.e., the dashed line indicates 3π displacement here) nucleating in the wake of the propagating wall (a). The loops grow transversely (b) eventually forming a double layer behind the primary wall.

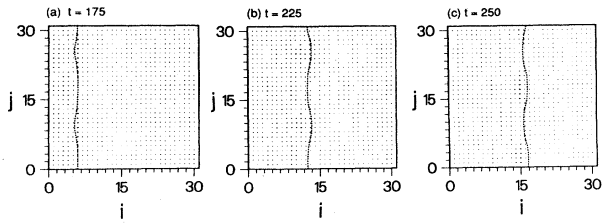

FIG. 6. A less discrete longitudinal lattice ($K_L=0.405$) and $\hat{F}=0.9$. Here two kink-antikink pairs are nucleated and sustain persistent transverse propagation.

IV. CONCLUSION

In this study we have used numerical simulations to examine the transverse structure generated on a moving wall in a 2D, longitudinally discrete Frenkel-Kontorova model with uniaxial displacements. The structures we have observed are generated by the nucleation of kink-antikink pairs. The Peierls-Nabarro barrier (arising from longitudinal lattice discreteness) plays a dominant role in the nucleation of such structures. Clearly the phenomenon does not occur in a continuum model since then the Peierls-Nabarro barrier vanishes. In addition, the driving force is important for the phenomenon, since this must be sufficiently strong to place the wall dynamics in an inhomogeneous depinning regime. Similarly, dissipation must be sufficiently weak. Too large a driving force nucleates additional (4π) kink-antikink pairs behind the primary wall, arising from *longitudinal* wall-shape oscillations.

In the present model, two characteristic lengths are important: The first is the longitudinal wall thickness, determined by the magnitude of the Peierls-Nabarro barrier via the longitudinal coefficient K_L [see Eq. (8b) for the definition of the strength of the Peierls-Nabarro barrier]; the second length characterizes the width of the transverse structure and is determined by the transverse lattice coefficient K_T [see Eq. (21) for the definition of this width]. Note that if K_T is too small, resulting in narrow transverse thicknesses, the transverse structure may itself be trapped on the lattice and inhibit transverse (and therefore longitudinal) dynamics. As shown by our collective coordinate reduction (Sec. II), the ratio of the applied force to the strength of the Peierls-Nabbaro barrier is important in order to place the effective force $\hat{F}$ in the right range for transverse instabilities. Thus, the anisotropy of the medium (via K_T/K_L) is essential within the present system. However, other circumstances creating a periodic potential in which the wall moves will also induce similar transverse instabilities—e.g., periodic, spatially homogeneous ac driving[12,19] or parametric space variations.[3] Similarily, whereas 1D models[13] (see Sec. II) appear to be good pardigms for wall propagation in 2D, the same argument generalizes to general D, although with different saturated nonlinear patterns. Thus, transverse nucleation on walls propagating in a 3D lattice are expected to appear as 2D patterns.

Related instabilities are also to be expected with other

transverse boundary conditions, e.g., periodic modulo a fixed phase difference. Examples include the underdamped motion of incommensurate arrays of discommensuration walls (e.g., in incommensurate lattices of charge-density-wave systems) where depinned discommensurations (Ref 20) will move by transverse propagation of kinks; nucleation and growth of new incommensurate structures by transverse modulation;[21] instabilities on odd zero-field steps (e.g., one fluxon), in annular Josephson junctions.[18] Similar problems occur in hydrodynamics, as in the convection of anisotropic fluids (e.g., nematic liquid crystals). There[22] convective flow can give rise to spatio-temporal structures, including transversally modulated patterns, zig-zag shapes and chaotic patterns, as the control parameter is slowly changed. Applications to these and other contexts mentioned in Sec. I will be examined elsewhere.

ACKNOWLEDGMENTS

Two of us (S. A. and J. P.) acknowledge the hospitality of the Center for Nonlinear Studies and the Theoretical Division at the Los Alamos National Laboratory. This work was supported by the U.S. Department of Energy.

APPENDIX A: EQUATION FOR THE WALL LOCATION

In this appendix we derive an approximate equation for the wall location in the case of a wall moving in a three-dimensional lattice with damping and dc driving. We start with the Lagrangian defined by Eq. (2) in which the change of variables and notations given by Eqs. (4a) and (4b) have been used. The Lagrangian is

$$\mathcal{L}=\int_{\mathbb{R}^2}\left\{\sum_i\left[\tfrac{1}{2}(\Phi_{i,\tau})^2-\tfrac{1}{2}(\Phi_{i+1}-\Phi_i)^2-\tfrac{1}{2}\left[\frac{\partial\Phi_i}{\partial x}\right]^2-\tfrac{1}{2}\left[\frac{\partial\Phi_i}{\partial y}\right]^2-\lambda(1-\cos\Phi_i)\right]\right\}dx\,dy\ . \tag{A1}$$

Now, we force the ansatz defined by Eqs. (6a)–(6d) to satisfy the variational principle associated with the Lagrangian (A1). Assuming the existence of the function $\Phi_i(x)$ of the discrete variable i and continuous variables x, and y, we can rewrite the Lagrangian density in the form

$$\mathcal{L}=\tfrac{1}{2}\mu^2[(U_\tau)^2-(U_x)^2-(U_y)^2-1-\lambda/\mu^2]\sum_i(g_i)^2\ , \tag{A2}$$

with

$$g_i=\frac{2}{\cosh(\mu\xi_i)}=\frac{\partial\Phi_i}{\partial(\mu\xi_i)}\ . \tag{A3}$$

The function

$$F(U)=\sum_i(g_i)^2$$

is one periodic $[F(U+1)=F(U)]$, so that this function can be expanded in a Fourier series. After some manipulation we obtain

$$\sum_i(g_i)^2=\frac{8}{\mu}\left[1+\tfrac{1}{2}\sum_{n=1}^{\infty}I(n)\cos(2\pi nU)\right]\ , \tag{A4}$$

where $I(n)$ is given by

$$I(n)=-\frac{8\pi^2 n}{\mu\sinh(\pi^2 n/\mu)}\ . \tag{A5}$$

We keep only the first-order term in (A4). Then, if the wall velocity is sufficiently small, we can write the Lagrangian to second order in the wall velocity. This yields

$$\mathcal{L}=E(0)\int_{\mathbb{R}^2}[\tfrac{1}{2}(U_\tau)^2-\tfrac{1}{2}(U_x)^2-\tfrac{1}{2}(U_y)^2-A(1-\cos2\pi U)]dx\,dy\ , \tag{A6a}$$

with

$$E(0)=8\sqrt{\lambda}\ , \tag{A6b}$$

$$A=\frac{4\pi^2}{\sqrt{\lambda}\sinh(\pi^2/\sqrt{\lambda})}\ . \tag{A6c}$$

$E(0)$ represents the rest energy of the wall.

In the presence of dissipation and driving, the variational principle must include the generalized force associated with the damping and the driving force. The total virtual work connected with the damping force is

$$\delta W_D=-\sum_i\Gamma\Phi_{i,\tau}\delta\Phi_i=-\left[\Gamma\mu^2U_\tau\sum_i(g_i)^2\right]\delta U=Q_D\delta U\ , \tag{A7}$$

where $\delta\Phi_i$ and δU are the variations associated with the displacement field Φ_i and wall location U, respectively. Q_D is the generalized damping force associated with the motion of the wall location

$$Q_D=-\Gamma E(0)U_\tau\ . \tag{A8}$$

The virtual work from the driving force is

$$\delta W_F=-\left[G\mu\sum_i g_i\right]\delta U \tag{A9}$$

and the effective force acting on the motion of the wall location is given by

$$Q_F=-2\pi G\ . \tag{A10}$$

The variational principle associated with the wall location U leads to the following equation:

$$U_{\tau\tau}-U_{xx}-U_{yy}+\pi A\sin(2\pi U)=-\Gamma U_\tau-\frac{\pi}{4\sqrt{\lambda}}G\ . \tag{A11}$$

Then, using the notations (8a)–(8c), Eq. (A11) transforms into Eq. (7).

APPENDIX B: FLOQUET ANALYSIS OF THE PARAMETRIC INSTABILITY

Equation (13a) can be rewritten as

$$\begin{aligned} x &= v \ , \\ v &= -2bv - [\omega_1^2 + b^2 + a(\omega_0 t)]x \ , \end{aligned} \tag{B1}$$

where it is straightforward to establish the connection with the notation used in Sec. II. $a(x)$ is a 2π periodic function with zero average and is supposed to be small. Let $x(t)$ be a solution of Eq. (B1) then $x(t+T)$ with $T=2\pi/\omega_0$ is also a solution. Since the space of solutions of Eq. (B1) is a two-dimensional vectorial space, there exists a linear operator F, independent of t, such that

$$\begin{bmatrix} x(T) \\ v(T) \end{bmatrix} = \underline{F} \begin{bmatrix} x(0) \\ v(0) \end{bmatrix} . \tag{B2a}$$

The matrix of this operator is called the Floquet matrix which maps the solution at 0 onto the solution at (nT) for integer n ,

$$\begin{bmatrix} x(nT) \\ v(nT) \end{bmatrix} = \underline{F}^n \begin{bmatrix} x(0) \\ v(0) \end{bmatrix} . \tag{B2b}$$

If the eigenvalues of $\underline{F}$ both have modulus smaller or equal to one, the solutions of Eq. (B1) are stable. Conversely, if one of the eigenvalues of $\underline{F}$ has modulus greater than one, the solution of Eq. (B1) is then unstable.

The procedure to estimate the eigenvalues of $\underline{F}$ is to consider a perturbation with respect to $a(x)$. For $a(x)=0$ it is easy to obtain the Floquet matrix since the system (B1) reduces to a linear system of equations. When $a(x)\neq 0$, the Floquet matrix can be calculated by considering the system (B1) with discretized time, and we can write

$$\begin{bmatrix} x_{n+1} \\ v_{n+1} \end{bmatrix} = [\underline{I} + \Delta t \underline{P}(n\Delta t)] \begin{bmatrix} x_n \\ v_n \end{bmatrix} , \tag{B3a}$$

where we have set

$$\underline{P}(t) = \begin{bmatrix} 0 \\ -[\omega_1^2 + b^2 + a(t)] - 2b \end{bmatrix} , \tag{B3b}$$

and $x_n = x(n\Delta t)$ with $\Delta t = T/N$. Now the Floquet matrix can be obtained as the limit of an infinite matrix product

$$\underline{F} = \lim_{N\to\infty} \prod_{n=1}^{N} \left[\underline{I} + \frac{T}{N} \underline{P}\left[\frac{nT}{N} \right] \right] , \tag{B4}$$

where $\underline{I}$ is the 2×2 unit matrix. From Eq. (B4) the determinant of the Floquet matrix is

$$D = \det \underline{F} = \lim_{N\to\infty} \left[1 - 2b\frac{T}{N} \right]^N = e^{-2bT} . \tag{B5}$$

It is sufficient to calculate the trace of the Floquet matrix. We expand the Floquet matrix [to second order in $a(x)$ with $N\to\infty$] around the zeroth-order Floquet matrix $\underline{F}_0$ obtained for $a(x)=0$ After some calculation we arrive at

$$S = \mathrm{Tr}\underline{F} = e^{-bT} \left[2\cos\omega_1 T + \frac{T}{2\omega_1^2} \sin\omega_1 T \sum_n \frac{a_n a_{-n}}{n\omega_0 + 2\omega_1} \right] , \tag{B6}$$

where the a_n's are the coefficients of the Fourier expansion of a $a(x)$. Since we are interested in an instability condition, we suppose that

$$\frac{2\omega_1}{\omega_0} = p + \varepsilon , \tag{B7}$$

where p is an integer and ε is a small parameter. This means that we are very close the parametric resonance condition. On substituting (B7) and (B6) and taking the limit $\epsilon\to 0$ we obtain

$$S = (-1)^p 2e^{-bT} \left[1 + \frac{2\pi^2}{\omega_0^2 p^2} |a_p|^2 \right] . \tag{B8}$$

Then, the eigenvalues of the Floquet matrix are both real and are the roots of the equation $x^2 - Sx + D = 0$. The latter must be negative for $x = (-1)^p$ in order ot fulfill the instability condition. Thus $1 - S(-1)^p + D < 0$. Using Eqs. (B5) and (B8) for small b, this condition becomes

$$\frac{b^2 T^2}{2} < \frac{2\pi^2}{\omega_0^4 p^2} |a_p|^2 . \tag{B9}$$

The instability condition at the order p in Eq. (B1) is satisfied when the damping constant b satisfies

$$b < \frac{|a_p|}{|p|\omega_0} . \tag{B10}$$

Validity for this perturbative scheme requires that the perturbation of S with respect to ϵ in comparison to $2(-1)^p e^{-bT}$, viz.,

$$\frac{\pi\sqrt{2}}{\omega_0^2 p} |a^p| \ll 1 . \tag{B11}$$

---

*Permanent address: Laboratoire de Mécanique Théorique, Université Pierre et Marie Curie, Tour 66, 4 place Jussieu, 75252 Paris CEDEX 05, France.

†Permanent address: Laboratoire Leon Brillouin, C.E.N. Saclay, F-91191, Gif-sur-Yvette CEDEX, France.

[1]For example, *Fronts, Interfaces and Patterns,* edited by A. R. Bishop, L. J. Campbell, and P. J. Channel (North-Holland, Amsterdam, 1983), or Physica **12D**, 1 (1984).

[2]For example, *Proceedings of the Conference on Charge Density Waves in Solids, Budapest, 1984,* Vol. 217 of *Lecture Notes in Physics* (Springer-Verlag, New York, 1985).

[3]For example, P. Martinoli, Phys. Rev. B **17**, 1173 (1978).

[4]J. W. Cahn, Acta Metall. **8**, 554 (1960).

[5]F. C. Franck and J. H. Van der Merwe, Proc. R. Soc. London

Ser. A **198**, 205 (1949); **201**, 261 (1950).
[6]M. Peyrard and M. D. Kruskal, Physica **14D**, 88 (1984).
[7]J. A. Combs and S. Yip, Phys. Rev. B **28**, 2566 (1983).
[8]C. Willis, M. El-Batonouny, and P. Stanicoff, Phys. Rev. B **33**, 1904 (1986).
[9]P. Stancioff, C. Willis, M. El-Batonouny, and S. Burdick Phys. Rev. B **33**, 1912 (1986).
[10]St. Pnevmatikos, M. Remoissenet, and N. Flytzanis, Phys. Rev. B **33**, 2308 (1986).
[11]M. Remoissenet, Phys. Rev. **33**, 2386 (1986).
[12]O. H. Olsen, P. S. Lomdahl, A. R. Bishop and J. C. Eilbeck, J. Phys. C **18**, L511 (1985).
[13]J. C. Ariyasu and A. R. Bishop, Phys. Rev. B **35**, 3207 (1987).
[14]S. Aubry, in *Solitons and Condensed Matter,* edited by A. R. Bishop and T. Schneider (Springer-Verlag, Berlin, 1978).
[15]M. Peyrard and S. Aubry, J. Phys. C **16**, 1593 (1983).
[16]S. Aubry, Physica **7D**, 240 (1983).
[17]P. S. Lomdahl and D. J. Srolovitz, Phys. Rev. Lett. **21**, 2702 (1986); Physica **16D**, 402 (1986).
[18]For example, A. Davidson, M. F. Pedersen, and S. Pagano, Appl. Phys. Lett. **48**, 1306 (1986).
[19]A. R. Bishop and P. S. Lomdahl, Physica **18D**, 54 (1986); A. R. Bishop *et al., ibid.* **23D**, 293 (1986).
[20]S. Aubry and L. de Seze, Festkörperprobleme **XXV**, 1 (1985).
[21]For example, K. Parlinski, Phys. Rev. B **35**, 8680 (1987).
[22]A. Joets and R. Ribotta, J. Phys. (Paris) **47**, 595 (1986).